BMP4 regulates the hematopoietic stem cell niche

Devorah C. Goldman,[1] Alexis S. Bailey,[1] Dana L. Pfaffle,[1] Azzah Al Masri,[1] Jan L. Christian,[2] and William H. Fleming[1,2]

[1]Department of Medicine, Division of Hematology and Medical Oncology, Oregon Stem Cell Center and Knight Cancer Institute, and [2]Department of Cell and Developmental Biology, Oregon Health & Science University, Portland

Bone morphogenetic protein 4 (BMP4) is required for mesoderm commitment to the hematopoietic lineage during early embryogenesis. However, deletion of BMP4 is early embryonically lethal and its functional role in definitive hematopoiesis is unknown. Consequently, we used a BMP4 hypomorph to investigate the role of BMP4 in regulating hematopoietic stem cell (HSC) function and maintaining steady-state hematopoiesis in the adult. Reporter gene expression shows that *Bmp4* is expressed in cells associated with the hematopoietic microenvironment including osteoblasts, endothelial cells, and megakaryocytes. Although resting hematopoiesis is normal in a BMP4-deficient background, the number of c-Kit$^+$, Sca-1$^+$, Lineage$^-$ cells is significantly reduced. Serial transplantation studies reveal that BMP4-deficient recipients have a microenvironmental defect that reduces the repopulating activity of wild-type HSCs. This defect is even more pronounced in a parabiosis model that demonstrates a profound reduction in wild-type hematopoietic cells within the bone marrow of BMP4-deficient recipients. Furthermore, wild-type HSCs that successfully engraft into the BMP4-deficient bone marrow show a marked decrease in functional stem cell activity when tested in a competitive repopulation assay. Taken together, these findings indicate BMP4 is a critical component of the hematopoietic microenvironment that regulates both HSC number and function. (Blood. 2009;114:4393-4401)

Introduction

Bone morphogenetic protein 4 (BMP4), a member of the transforming growth factor-β superfamily of secreted signaling molecules, regulates cell proliferation differentiation, apoptosis, and cell fate determination throughout mammalian development.[1-3] Hematopoietic cells are among several tissues that are dependent upon BMP4 in the embryo.[4] Specifically, BMP4 regulates mesodermal cell commitment to the hematopoietic lineage such that in embryos lacking BMP4, primitive hematopoiesis fails to occur.[3] Later during embryogenesis, BMP4 is expressed in the aorta-gonad-mesonephros region (AGM), where nascent hematopoietic stem cells (HSCs) emerge.[5-7] Recent experimental evidence indicates that BMP4 is part of a functional microenvironment that supports these nascent HSCs. Addition of BMP4 to cell cultures enriched for AGM-derived HSCs increases their hematopoietic colony-forming capability,[7] and blocking of BMP signaling abrogates HSC repopulating activity of AGM cultures.[5] Further evidence that BMP4 supports definitive HSCs comes from analysis of CD34$^+$CD38$^-$ HSC-enriched human cord blood cells cultured in the presence of BMP4. BMP4 increases CD34$^+$CD38$^-$ cell colony-forming activity as well as the repopulating activity of CD34$^+$CD38$^-$ cells in nonobese diabetic/severe combined immunodeficient recipients.[8,9]

Despite the evidence that exogenous BMP4 can influence adult HSC maintenance, there is little in vivo evidence to support this possibility. BMP4 knockout mice die early in embryogenesis and, to date, tissue-specific knockouts that can address the requirement of BMP4 for definitive HSC function have not been reported. Recently, we created a mouse in which a point mutation decreases the amount of mature BMP4 ligand available for signaling in a tissue-specific manner.[10] These mice, referred to as *Bmp4*$^{S2G/S2G}$, are viable hypomorphs. Apart from a failure to maintain spermatogenesis in approximately 50% of males, *Bmp4*$^{S2G/S2G}$ mice have no other gross defects.[10,11] For this study, we exploited these BMP4 hypomorphic mice to determine whether BMP4 is required for adult hematopoiesis and HSC activity. Our results indicate that *Bmp4* is expressed in several cell types associated with the hematopoietic microenvironment. BMP4 deficiency causes a reduction in the number of c-kit$^+$, Sca-1$^+$, Lin$^-$ (KSL) cells due to a cell-extrinsic defect. Serial transplantation and parabiosis studies show that BMP4 deficiency in the microenvironment impairs the functional activity of normal HSCs.

Methods

Mice

Bmp4$^{S2G/S2G}$ CD45.2 mice were genotyped as described[10] and were backcrossed for a minimum of 6 generations to C57BL/6J before analysis. *Bmp4*$^{lacZ/+}$ mice were obtained from Dr B. Hogan (Duke University, Durham, NC) and genotyped as described.[12] CD45.1 C57BL/6J and CD45.2 C57BL/6J mice were purchased from The Jackson Laboratory, and C57BL/6 TgN(act-EGFP)OsbY01 mice were provided by Dr Masaru Okabe (Osaka University, Osaka, Japan). CD45.1 C57BL/6J and CD45.2 C57BL/6J mice were intercrossed to generate CD45.1/CD45.2 hybrids. All mice were maintained in a breeding colony in the animal care facility at the Oregon Health & Science University. All procedures were approved by the Institutional Animal Care and Use Committee of the Oregon Health & Science University.

Submitted February 18, 2009; accepted August 24, 2009. Prepublished online as *Blood* First Edition paper, September 16, 2009; DOI 10.1182/blood-2009-02-206433.

The online version of this article contains a data supplement.

The publication costs of this article were defrayed in part by page charge payment. Therefore, and solely to indicate this fact, this article is hereby marked "advertisement" in accordance with 18 USC section 1734.

In situ BMP4 expression analysis

For β-galactosidase activity detection, isolated bones from 6- to 12-week-old *Bmp4*$^{lacZ/+}$ and wild-type (WT) controls were fixed for 1 hour in 4% paraformaldehyde and then decalcified in 14% EDTA (ethylenediaminetetraacetic acid, pH 7.2) until pliable. The bones were washed and stained in bromo-chloro-indolyl-galactopyranoside substrate, and subsequently embedded in paraffin, sectioned, and counterstained with eosin. To detect β-galactosidase protein, long bones were processed for frozen sections by fixing for 24 hours in 4% paraformaldehyde in phosphate-buffered saline, followed by 14% EDTA, which was changed daily for a total of 5 to 7 days. The bones were then dehydrated in 30% sucrose/phosphate-buffered saline overnight, embedded in OCT compound (Sakura Finetek), and cryosectioned. Sections were blocked using the avidin/biotin blocking kit (Vector Laboratories) and/or IMAGE-iT (Invitrogen) and stained overnight at 4°C with 1:500 rabbit anti–β-galactosidase (Immunology Consultants Laboratory) and 1:50 rat anti–platelet endothelial cell adhesion molecule-1 (BD Pharmingen). Secondary antibodies (1:400) conjugated to Alexa Fluor 488 (Invitrogen), cyanine3 (Cy3), or Cy5 (Chemicon) were used. All immunofluorescently stained sections were counterstained with DAPI (4,6 diamidino-2-phenylindole) to visualize nuclei and mounted in FluoromountG (SouthernBiotech).

Bromo-chloro-indolyl-galactopyranoside–stained sections were photographed with a Nikon Optiphoto2-UD microscope equipped with a 20×/0.50 objective lens and used in conjunction with a Nikon DXM 1200F digital camera and Nikon Act-1 Version 2.62 imaging software. Sections stained for immunofluorescence were photographed with a Zeiss Axiophot 200 microscope using a 40×/0.60 Zeiss Achroplan objective, a true color AxioCam camera or a monochromatic AxioCam camera and standard epifluorescence filters for fluorescein isothiocyanate (FITC), Cy3, Cy5, and DAPI (Carl Zeiss). Fluorescent images were digitally combined using Axio Vision software (Carl Zeiss).

Western analysis

For detection of BMP4 in bone marrow, cell extracts were prepared by sonication in radioimmunoprecipitation assay buffer (50 mM Tris [tris(hydroxymethyl)aminomethane], pH 8; 150 mM NaCl; 0.1% sodium dodecyl sulfate [SDS], 1% nonidet P-40, 0.5% sodium deoxycholate, 1× Roche mini complete protease inhibitor cocktail [Roche]). Samples were then incubated on ice for 20 minutes and centrifuged to remove cellular debris. Protein concentration was determined by bicinchoninic acid (BCA) analysis (Pierce), and 50 μg total protein for each sample was analyzed. For assessment of phosphorylated receptor Smads (Smad1, Smad5, and Smad8) in c-kit$^+$ bone marrow cells, equal numbers of cells were sorted from pairs of WT and mutant mice (2.4×10^5 cells per mouse and 3.2×10^5 cells per mouse in 2 independent experiments). Total protein was extracted by boiling samples in 1× SDS sample buffer (Santa Cruz Biotechnology) containing 2% β-mercaptoethanol as described by Utsugisawa et al.[13] Samples were separated by SDS–polyacrylamide gel electrophoresis and transferred to a polyvinylidene fluoride membrane. Blots were probed with goat anti-BMP4 antibody (1:500; Santa Cruz Biotechnology), rabbit anti-actin (1:10 000; Sigma-Aldrich), and/or rabbit anti–phospho-Smad1 (Ser463/465)/Smad5 (Ser463/465)/Smad8 (Ser426/428; 1:1000; Cell Signaling Technology) and rabbit anti-Smad1 (2 μg/mL; Upstate). After primary antibody incubation, blots were probed with horseradish peroxidase–conjugated secondary antibody (donkey anti–goat; Santa Cruz Biotechnology or donkey anti–rabbit; Amersham) and visualized by chemiluminescence.

Fluorescence-activated cell sorting

Donor bone marrow was prepared as previously described by Bailey et al.[14] All antibodies were purchased from BD Biosciences unless otherwise indicated. For KSL isolation, single-cell suspensions of bone marrow were labeled with antibodies to CD117 (c-kit)–allophycocyanin (APC) or c-kit–APC–Alexa Fluor 750 (eBioscience), Ly6 A/E (Sca-1)–FITC or Ly6 A/E–phycoerythrin (PE)–Cy7, and a PE–conjugated lineage mixture (B220, CD3, CD5, CD4, CD8, Mac1, Gr1, Ter119). KSL cells were enriched to homogeneity by double sorting c-kit$^+$/Sca-1$^+$/Lineage$^-$ cells using a FACSVantage or an Influx (both from Becton Dickinson). For isolation of c-kit$^+$ cells for Western blot analysis, single-cell suspensions were stained with CD117-APC and FACS sorted. Dead cells were excluded by a combination of scatter gates and propidium iodide staining.

Hematopoietic progenitor assays

Nucleated bone marrow cells (10^4) from WT and mutant mice were plated in triplicate in Methocult GF methylcellulose (M3434; StemCell Technologies) and incubated at 37°C. Erythroid burst-forming units (BFU-Es) were scored at 7 to 10 days and all other colonies were scored at 12 to 14 days.

Transplantation studies

Recipient mice (8-12 weeks old) were treated with a total dose of 1050 to 1200 cGy from a cesium irradiator administered in 2 equal doses delivered 3 hours apart. Donor cells were injected intravenously into the retro-orbital plexus in a total volume of 200 μL. Recipients received antibiotic water for 1 month after transplantation (neomycin sulfate at 1.1 g/L and polymyxin B sulfate at 167 mg/L).

Parabiosis

Parabiotic pairs of 6- to 12-week-old age- and weight-matched female CD45.1 WT or CD45.1 Y01 GFP$^+$ and CD45.2 *Bmp4*$^{S2G/S2G}$ mice were generated as previously described.[15] Two to 3 weeks after joining, each parabiotic mouse was given recombinant human granulocyte colony-stimulating factor (250 mg/kg, subcutaneously) for 4 days. Parabiotic mice were separated 8 weeks after joining.

Hematopoietic engraftment and complete blood count analysis

Peripheral blood leukocytes were obtained after erythrocyte depletion by sedimentation in 3% dextran (Amersham Pharmacia) and hypotonic lysis. Bone marrow was obtained by flushing tibia and femora. Multilineage hematopoietic engraftment was analyzed with antibodies to CD45.1 conjugated to PE or PE-Cy7 (eBioscience) and CD45.2 conjugated to FITC or APC–Alexa Fluor 750 (eBioscience) and the lineage markers Mac1-APC, Gr1-APC, B220-APC, and CD3-APC as previously described.[16] Cells were analyzed on a BD FACSCalibur or a BD LSRII (BD Biosciences) and data were analyzed using FCS express V3 (De Novo). Complete circulating blood analysis of peripheral blood was performed by Antech Diagnostics and IDEXX Laboratories.

Cell cycle and apoptosis analysis

To assess cell cycle, KSL cells from 8- to 12-week-old mice were double sorted from bone marrow, incubated overnight at 4°C in 70% ethanol containing 20 μg/mL propidium iodine, and then analyzed on a BD LSRII to measure DNA content. To assess apoptosis, simultaneous staining with annexin V–FITC, c-kit–APC, Sca-1–PE–Cy7, Lin-PE, and 7-amino-actinomycin-D (7-AAD) was performed on freshly isolated bone marrow and analyzed with a BD LSRII. Annexin V$^+$, 7-AAD$^-$ KSL cells were counted as apoptotic.

Statistical analysis

All quantitative experimental data were analyzed using the unpaired, 2-tailed Student *t* test. A *P* value less than .05 was considered significant.

Results

BMP4 is expressed in hematopoietic microenvironments

In the long bones, physical HSC niches and functional hematopoietic microenvironments have been identified in the endosteum, vasculature, and perivascular regions (reviewed by Kiel and Morrison[17]). To begin to determine whether BMP4 might be a

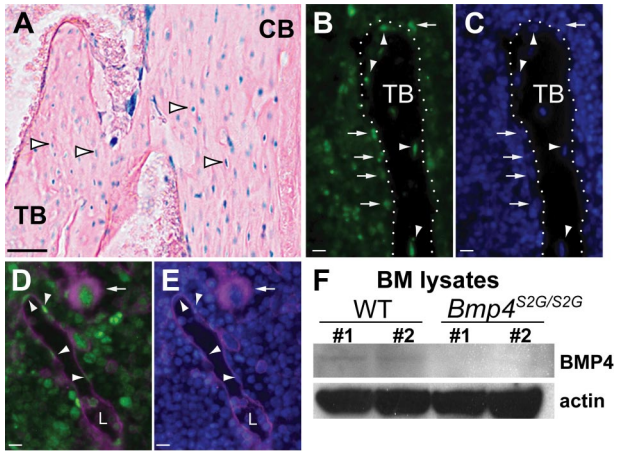

Figure 1. BMP4 is expressed in hematopoietic niches and BMP4 expression is reduced in the BM of *Bmp4*$^{S2G/S2G}$ mice. (A-E) Analysis of *Bmp4* expression in the long bones in *Bmp4*$^{lacZ/+}$ reporter mice. (A) β-Galactosidase enzyme activity (blue) is detected in the nuclei of trabecular (TB) and cortical (CB) bone-encased osteocytes (arrowheads), bone-lining cells, and BM cells. (B-C) Staining with (B) anti–β-gal antibody (green) and (C) DAPI (blue) confirms *Bmp4* is expressed in osteocytes (arrowheads) and bone-lining osteoblasts (arrows). Trabecular bone (TB) is outlined by the dotted white line. (D-E) CD31 and β-gal colocalize in the BM. (D) Merged image showing endothelial cells (arrowheads) and megakaryocytes (arrow) are among the BM cells costained with β-gal (green) and CD31 (magenta). L indicates blood vessel lumen. (E) Merged image showing DAPI (blue) and CD31 (magenta) expression. (F) Western analysis shows reduced levels of mature BMP4 (~ 24 kDa) expression in the BM of *Bmp4*$^{S2G/S2G}$ mice (n = 2) compared with WT controls (n = 2). Actin (~ 42 kDa) expression was probed as a loading control. Scale bars: (A) 80 μm, (B-E) 20 μm. See "In situ BMP4 expression analysis" for details about image acquisition and processing.

molecular regulator of the hematopoietic microenvironment, BMP4 expression was analyzed in the long bones of 6- to 12-week-old mice. Because of the technical difficulty encountered when trying to immunolocalize BMP4 in decalcified bone, we exploited a *Bmp4* knock-in reporter mouse,[12] which has been extensively used to identify *Bmp4*-expressing cells in both embryos and adults.[18-21] In this reporter line, exon 3 of *Bmp4* has been replaced with DNA encoding nuclear localized β-*galactosidase* (β-gal)*;* therefore*,* cells that express *Bmp4* mRNA display a nuclear β-gal signal. Strong β-gal enzyme activity was detected in cells lining the trabecular and cortical bone, osteocytes, and numerous bone marrow (BM) cells in *Bmp4*$^{lacZ/+}$ tibias and femurs, but not in age-matched *Bmp4*$^{+/+}$ controls (Figure 1A and data not shown).

Bmp4-expressing cells were further identified by coimmunolocalization of β-gal and the endothelial and hematopoietic[22] cell marker, CD31 (Figure 1B-E). This analysis confirmed that *Bmp4* is expressed in osteolineage cells (Figure 1B-C), vascular endothelial cells, and perivascular cells (Figure 1D-E). CD31 was also colocalized with β-gal in a subset of BM cells, including megakaryocytes (Figure 1D-E), which are also believed to support HSC/hematopoietic progenitors[23] and have been previously reported to express BMP4.[24]

We previously generated a *Bmp4* mutant allele *(Bmp4*^{S2G}*)* which causes a tissue-specific reduction in BMP4.[10] To determine whether levels of mature BMP4 ligand (~ 24 kDa) are reduced in the BM of *Bmp4*$^{S2G/S2G}$ mice, BMP4 expression in BM lysates was assessed by Western analysis. As shown in Figure 1F, significantly less mature BMP4 was detected in the BM from the hypomorphs. Together with the spatial analysis of the *Bmp4* reporter mice these data suggest that BMP4 is expressed appropriately to influence hematopoiesis and that BMP4 expression is significantly reduced in the BM of *Bmp4*$^{S2G/S2G}$ mice. Herein, we refer to *Bmp4*$^{S2G/S2G}$ mice as BMP4 hypomorphs or BMP4 mutants.

Table 1. Blood counts are normal in BMP hypomorphs

	WT	Mutant	*P*
WBCs, $\times 10^3/\mu L$	5.7 ± 1.1	9.7 ± 1.1	.03
RBCs, $\times 10^6/\mu L$	8.8 ± 0.2	9.1 ± 0.1	.21
Hemoglobin, g/dL	14.0 ± 0.4	14.6 ± 0.2	.12
Hematocrit, %	47.5 ± 1.8	52.5 ± 1.6	.06
MCV, fL	53.7 ± 1.1	57.2 ± 1.8	.20
MCH, pg	15.8 ± 0.1	16.0 ± 0.2	.57
MCHC, %	29.5 ± 0.8	27.9 ± 0.7	.21
Platelets, $\times 10^3/\mu L$	1147 ± 37	1171 ± 131	.86

Blood counts were assessed in 7 wild-type (WT) and 13 age-matched BMP4 hypomorphs (8-12 weeks old). Platelet counts were obtained for 5 WT and 5 BMP4 hypomorphs. All hematologic parameters measured for both genotypes were in the normal range. The mean value ± SEM is presented for each parameter. The calculated *P* values from unpaired, 2-tailed, Student *t* tests for each parameter are shown.

WBCs indicates white blood cells; RBCs, red blood cells; MCV, mean corpuscle volume; MCH, mean corpuscular hemoglobin; and MCHC, mean corpuscular hemoglobin concentration.

Resting hematopoiesis is normal in BMP4-deficient mice

To determine whether BMP4 is required for hematopoiesis under homeostatic conditions, numerous hematopoietic parameters were evaluated in 8- to 12-week-old BMP4 hypomorphs and age-matched wild-type controls. Circulating blood counts did not reveal any appreciable differences in total red cells, hematocrit, hemoglobin, or platelets (Table 1). Although circulating white blood cells (WBCs) were modestly increased in BMP4 hypomorphs, WBCs were within the normal range.[25]

Isolated hematopoietic cells from the spleen and bone marrow of 8- to 12-week-old mice were assessed for the frequency of hematopoietic lineages. For both of these hematopoietic organs, no significant differences in nucleated cell number were observed in BMP4 hypomorphs compared with WT controls (Figure 2A and data not shown). Notably, differences in gross bone morphology and length were not observed in whole and sectioned femurs from WT and mutant mice (data not shown). Flow cytometric analysis of the B-cell ($B220^+$), T-cell ($CD3^+$), red cell progenitor ($Ter119^+$), and myelomonocytic cell populations ($Mac1^+$ and/or $Gr1^+$) within the total $CD45^+$ hematopoietic population also revealed no significant differences between WT and mutants (Figure 2B). In total, these data indicate that resting hematopoiesis is normal in BMP4-deficient mice.

KSL number is reduced in BMP4 hypomorphs

BMP4 maintains $CD34^+CD38^-Lin^-$ human cord blood cell nonobese diabetic/severe combined immunodeficient repopulating activity as well as $CD34^+CD38^-Lin^-$ human cord blood cell proliferation and differentiation in a dose-dependent manner.[8,9] To further investigate BMP4 function in supporting adult HSCs in vivo, we assessed the frequency of HSC-enriched c-kit^+, Sca-1^+, $Lineage^-$ (KSL) cells present within the femurs of BMP4 hypomorphs compared with that of age- and sex-matched WT controls. As shown in Figure 3A and B, a 40% decrease in the absolute number of KSL cells per femur was detected in the BMP4 mutants. A similar decrease in the percentage of KSL cells in total nucleated femoral bone marrow cells was also observed.

To determine whether reduced BMP4 expression in the mutants affects BMP signaling in hematopoietic stem and progenitor cells, an antibody directed against the active, phosphorylated forms of the BMP pathway-specific Smads (Smad1, Smad5, and Smad8) was used for Western analysis of c-kit^+ cells isolated from WT and BMP4 hypomorphs. BM cells expressing c-kit are enriched for

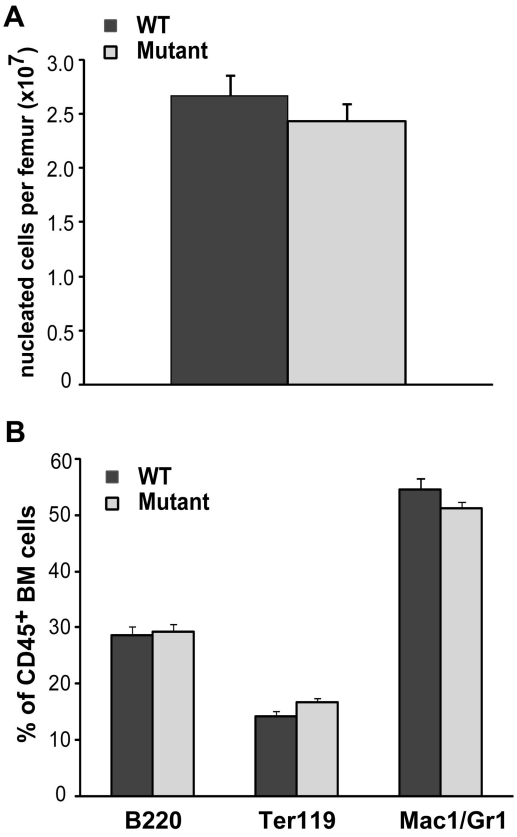

Figure 2. Resting hematopoiesis is normal in BMP4 hypomorphs. (A) The total number of nucleated bone marrow cells per femur in 8- to 12-week-old WT (n = 14) and BMP4 (n = 15) hypomorphs is not significantly different. (B) Hematopoietic lineage analysis in WT (n = 11) and BMP4 (n = 16) hypomorphs. The fractions of B cells (B220$^+$), red blood cell progenitors (Ter119$^+$), and myelomonocytic cells (Mac1/Gr1$^+$) within the CD45$^+$ BM population are shown. Error bars show SEM.

hematopoietic stem and progenitor cells. In 2 independent experiments, a significant reduction in phosphorylated Smad1/5/8, but not total Smad1/5, was detected in the hypomorphs (Figure 3C).

The KSL population is composed of both long-term and short-term HSCs that give rise to hematopoietic progenitors. We therefore assessed in vitro colony-forming activity in bone marrow to determine whether the frequency of committed myeloid hematopoietic progenitors is also altered in BMP4 hypomorphs. Specifically, the number and type of colony-forming units (CFUs), including erythroid (BFU-Es), granulocyte and/or macrophage (CFU-GM) and mixed myeloid lineage (granulocyte, erythroid, macrophage, megakaryocyte [CFU-GEMM]) were evaluated in methylcellulose cultures. Significant differences in total CFUs or in the frequency of each type of myeloid colony were not observed in the mutant bone marrow (Figure 3D). Our data therefore suggest that the HSC compartment may be specifically decreased in the setting of BMP4 deficiency.

To begin to understand how BMP4 regulates KSL cell maintenance, the cell cycle in KSL cells isolated from mutant and WT mice was assessed by measuring their DNA content. No difference in the proportion of cells in S/G2/M was detected in these populations in 5 independent experiments (Figure 3E). In some developmental contexts,[26,27] loss of BMP4 causes increased apoptosis. To determine whether the lack of BMP4 in the hypomorphs contributed to loss of KSL cells by inducing programmed cell death, the apoptotic fraction of KSL cells in BMP4 hypomorphs and WT mice was compared. Specifically, annexin V staining in these populations was assessed in 4 independent experiments. As shown in Figure 3F, no significant difference in the percentage of KSL cells undergoing apoptosis between mutant and WT cells was detected. Thus, a deficiency in BMP4 reduces KSL number without altering KSL cell cycle and apoptosis.

Wild-type HSCs lose functional activity in BMP4-deficient bone marrow

We hypothesized that the hematopoietic microenvironment is altered in BMP4 hypomorphs, thus accounting for the observed decrease in KSL cells. If this hypothesis is true, then wild-type HSCs placed into a mutant microenvironment should not be maintained as well as wild-type HSCs placed into a wild-type microenvironment. To test this, lethally irradiated 8- to 12-week-old mutant and WT CD45.2 mice were reconstituted with 10^5 CD45.1 WT bone marrow cells (Figure 4A). Long-term (> 24 weeks), high-level (> 90%), multilineage engraftment of primary recipient mice was confirmed by flow cytometric analysis of peripheral blood and BM (Figure 4B). To test the self-renewal activity of the donor HSCs, BM harvested from WT and mutant primary recipients after more than 24 weeks of engraftment was transplanted into lethally irradiated WT CD45.2 secondary recipients at a dose of 10^6 cells per mouse (Figure 4A). Flow cytometric peripheral blood (PB) analysis of the secondary recipients 20 weeks after transplantation revealed that WT donor cells that had passaged through a primary mutant host reconstituted hematopoiesis to a much lower extent (3.1-fold decrease; $P = .01$) compared with WT cells passaged through a WT host (Figure 4C). Thus, self-renewal activity of WT HSCs is compromised in BMP4-deficient mice. These data support our hypothesis that BMP4 is a critical component of the HSC microenvironment that regulates HSC in a non–cell-autonomous manner.

Parabiosis reveals that WT HSCs and progenitor cells engraft and function poorly in a BMP4-deficient microenvironment

In the irradiation model used for the transplantation experiments described in the previous section, there are many inductive signals that drive the engraftment and expansion of donor hematopoietic cells in the damaged and "empty" hematopoietic microenvironment. Therefore, the extensive regeneration seen after lethal irradiation and bone marrow transplantation in the primary recipients might initially compensate for and mask a microenvironmental defect present during steady-state hematopoiesis. We therefore wished to determine whether a microenvironmental defect exists in BMP4 hypomorphs under steady-state conditions.

To assay the functionality of the hematopoietic microenvironment in BMP4 hypomorphs without myeloablative preconditioning and in a competitive engraftment setting that more closely approximates steady-state conditions, we used a parabiotic model (Figure 5A). In this model, pairs of 6- to 12-week-old, age-matched WT (CD45.1 or CD45.1; Y01 GFP) and BMP4 hypomorphic (CD45.2) mice were surgically joined to establish cross circulation and trafficking of HSCs between each pair of mice. Two weeks after joining, granulocyte colony-stimulating factor was administered to mobilize HSCs from hematopoietic niches and encourage their engraftment into partner parabionts.[28] The parabionts were separated approximately 6 weeks later and donor-derived hematopoiesis was assessed at various time points. We hypothesized that if the hematopoietic microenvironment in the BMP4 hypomorph was defective, then both WT and mutant long-term repopulating cells would preferentially engraft in the WT parabiont. As a control, we

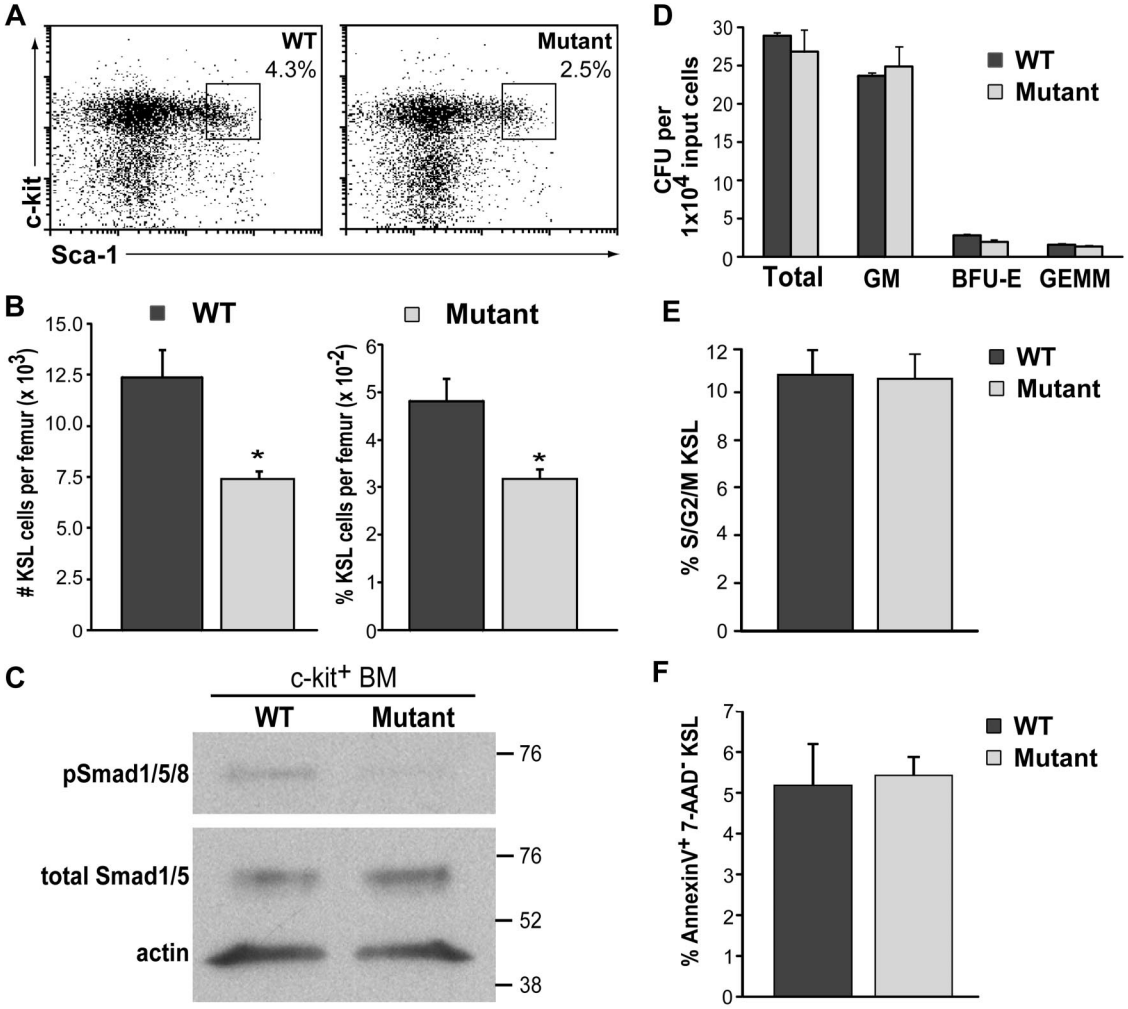

Figure 3. KSL number is reduced in BMP4 hypomorphs. (A) Representative FACS plots of c-kit$^+$/Sca-1$^+$/lin$^-$ (KSL) cells (boxed areas) isolated from 8- to 12-week-old WT and BMP4 hypomorphic mice. Live cells within the lineage-negative gate are shown. (B) Pooled data for total KSL number per femur (left) and the percentage of KSL cells per femur (right) are shown. Significantly fewer KSL cells are detected in the BMP4 hypomorphs (n = 15) relative to that in age-matched controls (n = 14). *$P < .004$. (C) Analysis of phosphorylated (p) Smad1/5/8 in sorted c-kit$^+$ BM cells from WT and mutant mice. In this representative Western blot, 2.4×10^4 cells from each genotype were assayed with an antibody that recognizes pSmad1, pSmad5, and pSmad8 (~ 60 kDa, top panel). The blot was stripped and reprobed (bottom panel) with antibodies that recognize total Smad1 and Smad5 (~ 60 kDa) and actin (~ 42 kDa). The positions of molecular weight markers (in kilodaltons) are indicated on the right. (D) Hematopoietic progenitor activity assays. Progenitor activity (colony-forming units [CFUs]) in 10^4 nucleated BM cells was assessed in methylcellulose cultures. Pooled data from 4 independent experiments performed in triplicate are shown. (E) KSL cell-cycle analysis. The fraction of sorted KSL cells in S/G2/M was determined for each genotype in 5 independent experiments. Significant differences in KSL cell cycle status between WT and mutant mice were not detected. (F) KSL apoptosis analysis. Pooled results from annexin V and 7-AAD staining of KSL cells from WT and BMP4 mutant mice. Four independent experiments were performed and no significant differences were detected. Error bars show SEM.

also generated congenic WT parabiotic pairs and mobilized and separated them on the same experimental schedule.

To quantitate the degree to which the mutant and WT hematopoietic microenvironments supported hematopoietic stem/progenitor cell engraftment and function, donor cell reconstitution of the blood was assessed in each parabiont 2 to 24 weeks after the mice had been separated. Multilineage, donor-derived hematopoiesis was detected at each time point (supplemental Figure 1, available on the *Blood* website; see the Supplemental Materials link at the top of the online article); however, as early as 2 weeks after separation (Figure 5B), we observed a significant decrease in the fraction of WT donor cells present in the blood of mutant hosts compared with the fraction of mutant cells detected in the blood of WT hosts (14.4% vs 33.8%; $P < .001$). Notably, in control WT/WT parabiotic pairs, donor cells comprise 32.6% of circulating leukocytes at this time point (Figure 5B). In the mutant/WT parabionts, a further reduction in circulating WT cells in mutant host peripheral blood was observed 24 weeks after separation compared with the fraction of circulating mutant cells present in WT hosts (7.1% vs 22.4%). In control WT/WT parabiosed mice, long-term donor cell hematopoiesis (22-30 weeks) in the blood (19.3%) was again very similar to the frequency of mutant cells in WT hosts. These results indicate that the BMP4-deficient environment minimally supports WT HSC function, whereas the WT microenvironment supports both mutant and WT HSCs to the same extent.

Consistent with these findings in the peripheral blood, analysis of donor cell engraftment in the bone marrow of 3 mutant/WT parabiotic pairs approximately 40 weeks after separation (Figure 5C) revealed minimal WT-derived hematopoiesis in mutant host BM, whereas mutant-derived blood cells were readily detected in WT host BM (1.9% vs 38.0%, $P < .006$). To rule out the possibility that WT hematopoietic cells preferentially homed to extramedullary hematopoietic sites in the BMP4 hypomorphs, we assessed donor cell frequency in the spleens in 2 of the parabiotic pairs. Similar to the results for the PB and BM, significantly fewer WT

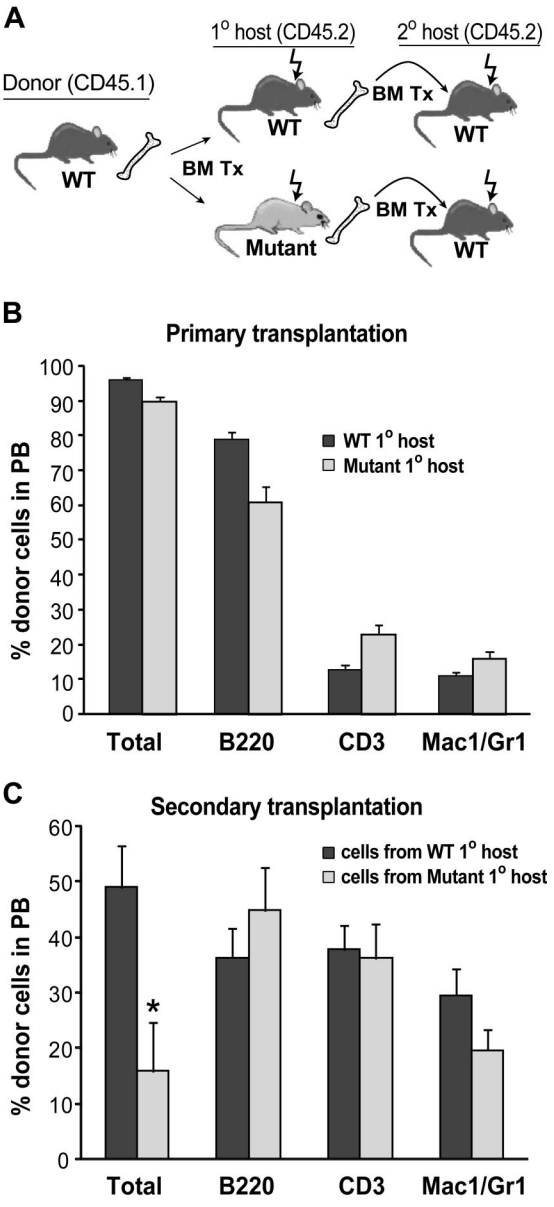

Figure 4. Reduction in WT HSC activity after transplantation into BMP4-deficient hosts. (A) Primary and secondary transplantation scheme. (B) Analysis of wild-type donor cell engraftment in WT (n = 6) and BMP4 (n = 6) hypomorphic primary recipients 24 weeks after transplantation. (C) Analysis of donor cell engraftment in secondary hosts 20 weeks after transplantation. Wild-type cells that engrafted into primary BMP4 hypomorphic hosts reconstituted long-term hematopoiesis in secondary recipients (n = 12) significantly less well than wild-type cells that engrafted into WT primary hosts before secondary transplantation (n = 9 secondary recipients). *$P = .01$. In panels B and C, total donor cells are shown as a percentage of live cells. Individual lineages are shown as the percentage of donor-derived cells. Error bars show SEM.

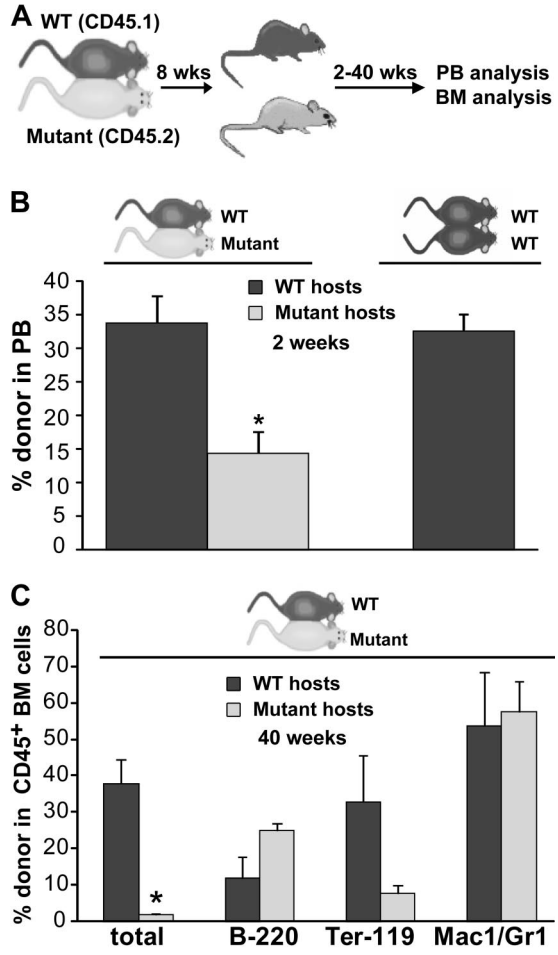

Figure 5. WT cells engraft poorly in BMP4-deficient mice after parabiosis. (A) Experimental strategy. (B) Donor cell analysis of the peripheral blood in mutant/WT parabiotic mice and WT/WT parabiotic mice 2 weeks after separation. Significantly fewer circulating WT donor cells are found in the mutant hosts after parabiosis (n = 7), whereas comparable donor engraftment of mutant donor cells into WT hosts (n = 6) or WT donor cells into WT hosts (WT/WT parabionts, n = 3) is observed. *$P < .001$. (C) BM donor cell engraftment and lineage analysis in 3 pairs of mutant/WT parabionts approximately 10 months after separation. Significantly fewer donor cells are observed in the mutant BM (*$P < .006$). Total donor cells are shown as a percentage of live cells. Individual lineages are shown as the percentage of donor-derived cells. Error bars show SEM.

cells (~ 6-fold) were detected in the spleens of the mutant hosts compared with the number of mutant cells that engrafted into WT hosts (data not shown).

As the low levels of WT reconstitutive activity in the mutant parabionts could simply reflect a bias against WT hematopoietic cell engraftment in a BMP4 hypomorph, we wished to directly ascertain whether WT cells that had successfully engrafted in the mutants possessed normal, long-term repopulating activity. Therefore, we FACS sorted equal numbers of donor CD45.1 WT BM cells and donor CD45.2 mutant BM from 3 pairs of mutant/WT parabionts (~ 40 weeks after separation) and transplanted them along with host type carrier cells into double congenic, 8- to 12-week-old CD45.1/CD45.2 host mice (Figure 6A). Assessment of long-term, multilineage engraftment of cells isolated from parabionts 16 weeks after transplantation revealed that WT donor cells isolated from the mutant parabiont hosts had severe defects in hematopoietic repopulating activity compared with equal numbers of mutant cells isolated from WT parabionts (Figure 6B; $P < .002$). In contrast, transplantation of equal numbers of host cells from the same WT and mutant parabiotic pairs (Figure 6C) revealed no significant difference in their long-term repopulating activity relative to each other (Figure 6D). These findings indicate that donor WT HSCs that had engrafted in the mutant mice lost reconstitutive activity as a result of prolonged contact with the BMP4-deficient hematopoietic microenvironment.

Discussion

Given the essential function of BMP4 in supporting embryonic hematopoiesis, it has been widely speculated that BMP4 regulates

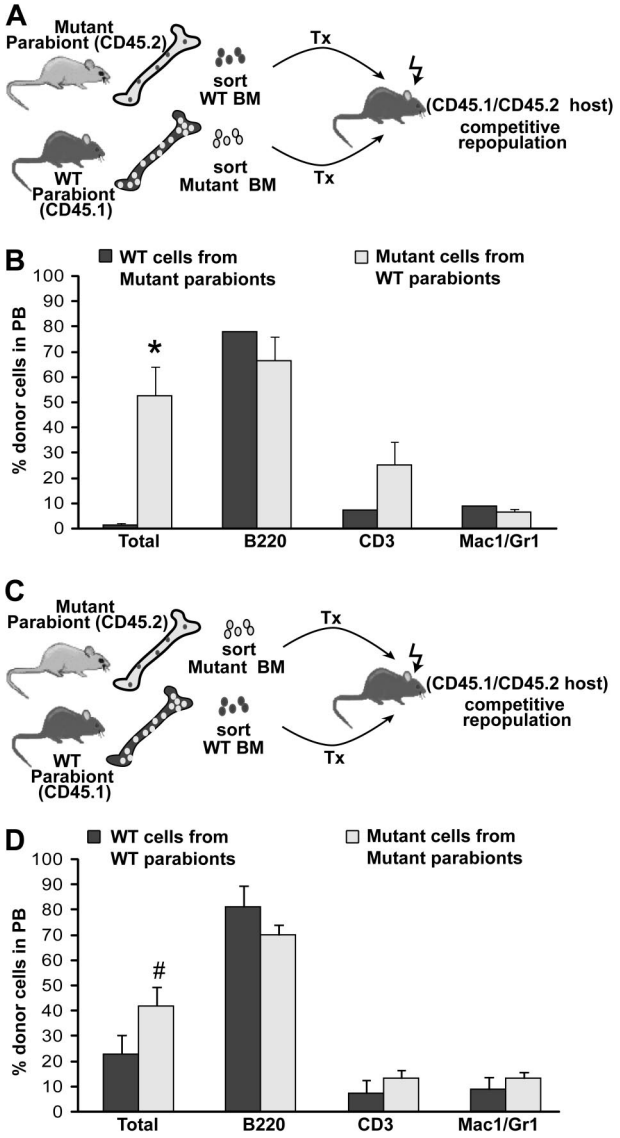

Figure 6. WT HSC activity is poorly supported in a BMP4-deficient microenvironment. (A) Approximately 10 months after separation, equal numbers of donor cells were FACS sorted from 3 pairs of mutant/WT parabionts and cotransplanted into secondary recipients along with an equal number of carrier BM cells. (B) Analysis of donor cell engraftment for the experiment diagrammed in panel A, 16 weeks after transplantation. WT cells conditioned in BMP4 hosts were drastically outcompeted by mutant cells conditioned in WT hosts. Two of a total of 5 secondary recipients were engrafted with WT cells. $*P < .002$. (C) To test host cell activity, equal numbers of host cells were also FACS sorted from 2 mutant/WT parabiont pairs approximately 10 months after separation and cotransplanted into secondary recipients along with an equal number of carrier BM. (D) Analysis of donor cell engraftment for the experiment diagrammed in panel C, 16 weeks after transplantation. Significant differences between WT and mutant cell engraftment were not detected, indicating comparable host cell activity. Four secondary recipients were assayed. $\#P = .12$. In panels B and D, total donor cells are shown as a percentage of live cells. Individual lineages are shown as the percentage of donor-derived cells. Error bars show SEM.

adult HSCs. Here, by exploiting a viable BMP4 hypomorphic mouse mutant in which BMP4 expression and signaling is reduced in the bone marrow, we have provided the first direct evidence that BMP4 signaling is necessary to maintain functional adult HSCs in vivo. Specifically, we have shown that BMP4 is expressed in several of the cell types that comprise the hematopoietic microenvironment. Adult mice deficient in BMP4 have significantly fewer KSL cells than wild-type mice, consistent with a decrease in HSC number. Furthermore, using serial transplantation, we have shown that wild-type HSCs transplanted into BMP4 mutants have a substantially reduced capacity for long-term hematopoietic repopulating activity. A parabiosis model revealed that circulating wild-type HSCs/progenitors engraft poorly in BMP4-deficient microenvironment, and that those few HSCs that do engraft lose a significant amount of their functional hematopoietic activity. Our data indicate that BMP4 is an important component of the HSC microenvironment and is necessary for maintaining HSC function.

Comparisons of the effects of exogenous BMP4 on human and mouse HSC cultures have revealed some notable differences in BMP4 activity in these populations. Whereas it has been previously demonstrated that BMP4 is sufficient to elicit a dose-dependent effect on the proliferation, CFU activity, and maintenance of primitive human $CD34^+CD38^-$ cells,[8,9] BMP4 has no measurable effect on cultured mouse BM-derived $CD34^-$KSL proliferation, CFU activity, or KSL expansion in vitro.[13] These discrepancies raise the possibility that BMP4 signaling in HSCs elicits different responses in different ontogenic sources of HSCs (eg, fetal cord blood vs adult long bones) and/or has species-specific functions in HSC regulation. Although our data suggest that BMP4 is required to maintain normal KSL number in vivo, we found that, as has been shown for mouse HSCs in vitro, changes in BMP4 signaling in vivo also do not alter KSL proliferation, KSL apoptosis (Figure 3F), KSL CFU activity (data not shown), and unfractionated BM CFU activity (Figure 3D), further underscoring the differences between human cord blood and adult mouse HSCs.

To regulate HSC functional activity, BMP4 may signal either directly or indirectly to HSCs. Numerous lines of evidence support direct signaling to HSCs and progenitors. First, purified KSL cells express the signaling machinery required to transduce a BMP4 signal, including the BMP type I receptor Alk2,[13,29] BMP-receptor activated Smads (Smad1 and Smad5), and the common Smad, Smad4.[13] Second, BMP4 is expressed appropriately within known HSC niches (Figure 1 and Sipe et al[24]). Finally, we have shown that in BMP4 hypomorphs, activation of BMP pathway–specific Smads is reduced in $c\text{-}kit^+$ BM, which is enriched for hematopoietic progenitors (Figure 3C).

The existing tissue-specific knockout mice in which BMP signaling components are deleted in HSCs do not provide conclusive evidence to discern whether BMP signaling directly regulates HSC function. Interestingly, loss of Smad4 in HSCs leads to impaired repopulating activity in vivo,[30] indicating that like BMP4, Smad4 is also essential for HSC maintenance. However, whether BMP signaling regulates Smad4 activity in HSCs is not yet clear. BMPs regulate Smad4 activity through activation of the receptor Smads, Smad1, Smad5, and Smad8. Whereas Smad8 is not expressed in HSCs,[13] and loss of Smad5 does not impact HSC function,[31] the effects of loss of Smad1 or Smad1 together with Smad5 in HSCs have not yet been reported. Furthermore, although Smad4 is the major transducer of BMP4 signals, recent findings highlight that other signaling pathways, such as the mitogen-activated protein kinase pathway, are activated in a Smad-independent manner.[32] Therefore, it remains to be determined whether and how BMP4 and other BMPs signal to HSCs.

Although direct BMP4 signaling to HSCs is an attractive possibility, BMP4 may mediate HSC function in an indirect manner. Specifically, BMP4 signaling may be necessary in another cell type(s) that in turn supports HSCs through the production of other cytokines and/or matrix factors. Based on our analysis of a *Bmp4* reporter mouse, *Bmp4* is expressed in or near bone-lining osteoblasts, endothelium, and perivascular cells, including megakaryocytes, and therefore, may be available to signal to all of these cell types. For instance, BMPs, which are known bone inducers, have complex functions in postnatal osteoblasts.[33-35] In some contexts, tissue-specific knockout of BmpR1a/Alk3[34] or overexpression of the BMP4 antagonist Noggin[36] reduces osteoblast function,

thereby resulting in bone loss. Whether such changes in osteoblast activity also impact hematopoiesis is presently unknown. Endothelial cells are also responsive to BMP4, as application of BMP4 to cultured microvascular endothelial cells can induce proliferation, migration, and angiogenesis.[37,38] Finally, recent data highlight an autocrine function of BMP4 in megakaryocyte differentiation.[39] Although we did not observe any obvious changes in femur architecture or morphology in the BMP4 mutants, further experiments are required to determine whether the niche function of any of these populations is adversely affected in *Bmp4*$^{S2G/S2G}$ mice.

BMP4 has been previously demonstrated to support HSC activity in nascent HSCs from the AGM region of embryonic day 11.5 embryos.[5] Our finding that BMP4 supports HSC maintenance in adult mice suggests that the HSC-supportive functions of BMP4 operate at all stages of definitive hematopoiesis. Whereas BMP4 supports HSC activity without affecting HSC number in the embryo, our data suggest that BMP4 maintains HSC number in adult bone marrow. Future studies will elucidate the precise mechanisms by which BMP4 maintains HSC number and activity in vivo.

Acknowledgments

We thank Dr B. L. M. Hogan for the *Bmp4*$^{lacZ/+}$ mice, and Dr L. Musil and B. Boswell for invaluable technical advice and assistance. We also thank the Oregon Health & Science University flow cytometry core for FACS.

This work was supported in part by a postdoctoral fellowship from the American Heart Association and by a grant from the National Institutes of Health (NIH; R03 HD056135) to D.C.G., by grant support from the Shriners' Hospital for Children Research Corporation, and a grant from the NIH (RO1 HD42598) to J.L.C., and by grants from the NIH (R01 HL077818 and R01 HL069133) to W.H.F.

Authorship

Contribution: D.C.G. designed experiments, performed research, analyzed and interpreted data, and wrote the manuscript; A.S.B., D.L.P., and A.A.M. performed experiments and analyzed data; J.L.C. provided vital reagents; and W.H.F. designed experiments, interpreted data, and wrote the manuscript.

Conflict-of-interest disclosure: The authors declare no competing financial interests.

Correspondence: Devorah Goldman, OHSU, 3181 SW Sam Jackson Park Rd, Mail Code L321, Portland, OR 97239; e-mail: goldmand@ohsu.edu.

References

1. Chen D, Zhao M, Harris SE, Mi Z. Signal transduction and biological functions of bone morphogenetic proteins. *Front Biosci.* 2004;9:349-358.
2. Chen D, Zhao M, Mundy GR. Bone morphogenetic proteins. *Growth Factors.* 2004;22(4):233-241.
3. Hogan BL. Bone morphogenetic proteins: multifunctional regulators of vertebrate development. *Genes Dev.* 1996;10(13):1580-1594.
4. Sadlon TJ, Lewis ID, D'Andrea RJ. BMP4: its role in development of the hematopoietic system and potential as a hematopoietic growth factor. *Stem Cells.* 2004;22(4):457-474.
5. Durand C, Robin C, Bollerot K, Baron MH, Ottersbach K, Dzierzak E. Embryonic stromal clones reveal developmental regulators of definitive hematopoietic stem cells. *Proc Natl Acad Sci U S A.* 2007;104(52):20838-20843.
6. Marshall CJ, Kinnon C, Thrasher AJ. Polarized expression of bone morphogenetic protein-4 in the human aorta-gonad-mesonephros region. *Blood.* 2000;96(4):1591-1593.
7. Marshall CJ, Sinclair JC, Thrasher AJ, Kinnon C. Bone morphogenetic protein 4 modulates c-Kit expression and differentiation potential in murine embryonic aorta-gonad-mesonephros haematopoiesis in vitro. *Br J Haematol.* 2007;139(2):321-330.
8. Bhardwaj G, Murdoch B, Wu D, et al. Sonic hedgehog induces the proliferation of primitive human hematopoietic cells via BMP regulation. *Nat Immunol.* 2001;2(2):172-180.
9. Bhatia M, Bonnet D, Wu D, et al. Bone morphogenetic proteins regulate the developmental program of human hematopoietic stem cells. *J Exp Med.* 1999;189(7):1139-1148.
10. Goldman DC, Hackenmiller R, Nakayama T, et al. Mutation of an upstream cleavage site in the BMP4 prodomain leads to tissue-specific loss of activity. *Development.* 2006;133(10):1933-1942.
11. Goldman DC, Donley N, Christian JL. Genetic interaction between Bmp2 and Bmp4 reveals shared functions during multiple aspects of mouse organogenesis. *Mech Dev.* 2009;126(3-4):117-127.
12. Lawson KA, Dunn NR, Roelen BA, et al. Bmp4 is required for the generation of primordial germ cells in the mouse embryo. *Genes Dev.* 1999;13(4):424-436.
13. Utsugisawa T, Moody JL, Aspling M, Nilsson E, Carlsson L, Karlsson S. A road map toward defining the role of Smad signaling in hematopoietic stem cells. *Stem Cells.* 2006;24(4):1128-1136.
14. Bailey AS, Jiang S, Afentoulis M, et al. Transplanted adult hematopoietic stems cells differentiate into functional endothelial cells. *Blood.* 2004;103(1):13-19.
15. Bailey AS, Willenbring H, Jiang S, et al. Myeloid lineage progenitors give rise to vascular endothelium. *Proc Natl Acad Sci U S A.* 2006;103(35):13156-13161.
16. Montfort MJ, Olivares CR, Mulcahy JM, Fleming WH. Adult blood vessels restore host hematopoiesis following lethal irradiation. *Exp Hematol.* 2002;30(8):950-956.
17. Kiel MJ, Morrison SJ. Uncertainty in the niches that maintain haematopoietic stem cells. *Nat Rev Immunol.* 2008;8(4):290-301.
18. Corriere MA, Rogers CM, Eliason JL, et al. Endothelial Bmp4 is induced during arterial remodeling: effects on smooth muscle cell migration and proliferation. *J Surg Res.* 2008;145(1):142-149.
19. Frank DB, Abtahi A, Yamaguchi DJ, et al. Bone morphogenetic protein 4 promotes pulmonary vascular remodeling in hypoxic pulmonary hypertension. *Circ Res.* 2005;97(5):496-504.
20. Jiao K, Kulessa H, Tompkins K, et al. An essential role of Bmp4 in the atrioventricular septation of the mouse heart. *Genes Dev.* 2003;17(19):2362-2367.
21. Kulessa H, Turk G, Hogan BL. Inhibition of Bmp signaling affects growth and differentiation in the anagen hair follicle. *EMBO J.* 2000;19(24):6664-6674.
22. Baumann CI, Bailey AS, Li W, Ferkowicz MJ, Yoder MC, Fleming WH. PECAM-1 is expressed on hematopoietic stem cells throughout ontogeny and identifies a population of erythroid progenitors. *Blood.* 2004;104(4):1010-1016.
23. Kopp HG, Rafii S. Thrombopoietic cells and the bone marrow vascular niche. *Ann N Y Acad Sci.* 2007;1106:175-179.
24. Sipe JB, Zhang J, Waits C, Skikne B, Garimella R, Anderson HC. Localization of bone morphogenetic proteins (BMPs)-2, -4, and -6 within megakaryocytes and platelets. *Bone.* 2004;35(6):1316-1322.
25. Peters LL, Cheever EM, Ellis HR, et al. Large-scale, high-throughput screening for coagulation and hematologic phenotypes in mice. *Physiol Genomics.* 2002;11(3):185-193.
26. Liu W, Selever J, Murali D, et al. Threshold-specific requirements for Bmp4 in mandibular development. *Dev Biol.* 2005;283(2):282-293.
27. Liu W, Selever J, Wang D, et al. Bmp4 signaling is required for outflow-tract septation and branchial-arch artery remodeling. *Proc Natl Acad Sci U S A.* 2004;101(13):4489-4494.
28. Abkowitz JL, Robinson AE, Kale S, Long MW, Chen J. Mobilization of hematopoietic stem cells during homeostasis and after cytokine exposure. *Blood.* 2003;102(4):1249-1253.
29. Hogan BM, Layton JE, Pyati UJ, et al. Specification of the primitive myeloid precursor pool requires signaling through Alk8 in zebrafish. *Curr Biol.* 2006;16(5):506-511.
30. Karlsson G, Blank U, Moody JL, et al. Smad4 is critical for self-renewal of hematopoietic stem cells. *J Exp Med.* 2007;204(3):467-474.
31. Singbrant S, Moody JL, Blank U, et al. Smad5 is

dispensable for adult murine hematopoiesis. *Blood.* 2006;108(12):3707-3712.

32. Nohe A, Keating E, Knaus P, Petersen NO. Signal transduction of bone morphogenetic protein receptors. *Cell Signal.* 2004;16(3):291-299.
33. Kamiya N, Ye L, Kobayashi T, et al. Disruption of BMP signaling in osteoblasts through type IA receptor (BMPRIA) increases bone mass. *J Bone Miner Res.* 2008;23(12):2007-2017.
34. Mishina Y, Starbuck MW, Gentile MA, et al. Bone morphogenetic protein type IA receptor signaling regulates postnatal osteoblast function and bone remodeling. *J Biol Chem.* 2004;279(26):27560-27566.
35. Zhang J, Niu C, Ye L, et al. Identification of the haematopoietic stem cell niche and control of the niche size. *Nature.* 2003;425(6960):836-841.
36. Tsumaki N, Yoshikawa H. The role of bone morphogenetic proteins in endochondral bone formation. *Cytokine Growth Factor Rev.* 2005;16(3):279-285.
37. Rothhammer T, Bataille F, Spruss T, Eissner G, Bosserhoff AK. Functional implication of BMP4 expression on angiogenesis in malignant melanoma. *Oncogene.* 2007;26(28):4158-4170.
38. Suzuki Y, Montagne K, Nishihara A, Watabe T, Miyazono K. BMPs promote proliferation and migration of endothelial cells via stimulation of VEGF-A/VEGFR2 and angiopoietin-1/Tie2 signalling. *J Biochem.* 2008;143(2):199-206.
39. Jeanpierre S, Nicolini FE, Kaniewski B, et al. BMP4 regulation of human megakaryocytic differentiation is involved in thrombopoietin signaling. *Blood.* 2008;112(8):3154-3163.